MEDICAL ROBOTS

A fully implantable device for intraperitoneal drug delivery refilled by ingestible capsules

Veronica Iacovacci[1,2,3†], Izadyar Tamadon[1,2†], Emanuele Federico Kauffmann[4], Stefano Pane[1,2], Virginia Simoni[1,2], Leonardo Marziale[1,2], Michele Aragona[5], Luigi Cobuccio[6], Massimo Chiarugi[6], Paolo Dario[1,2,7,8,9], Stefano Del Prato[5], Leonardo Ricotti[1,2], Fabio Vistoli[4], Arianna Menciassi[1,2]*

Creating fully implantable robots that replace or restore physiological processes is a great challenge in medical robotics. Restoring blood glucose homeostasis in patients with type 1 diabetes is particularly interesting in this sense. Intraperitoneal insulin delivery could revolutionize type 1 diabetes treatment. At present, the intraperitoneal route is little used because it relies on accessing ports connecting intraperitoneal catheters to external reservoirs. Drug-loaded pills transported across the digestive system to refill an implantable reservoir in a minimally invasive fashion could open new possibilities in intraperitoneal delivery. Here, we describe PILLSID (PILl-refiLled implanted System for Intraperitoneal Delivery), a fully implantable robotic device refillable through ingestible magnetic pills carrying drugs. Once refilled, the device acts as a programmable microinfusion system for precise intraperitoneal delivery. The robotic device is grounded on a combination of magnetic switchable components, miniaturized mechatronic elements, a wireless powering system, and a control unit to implement the refilling and control the infusion processes. In this study, we describe the PILLSID prototyping. The device key blocks are validated as single components and within the integrated device at the preclinical level. We demonstrate that the refilling mechanism works efficiently in vivo and that the blood glucose level can be safely regulated in diabetic swine. The device weights 165 grams and is 78 millimeters by 63 millimeters by 35 millimeters, comparable with commercial implantable devices yet overcoming the urgent critical issues related to reservoir refilling and powering.

INTRODUCTION

Medical robotics has evolved in recent years (*1*–*3*), with substantial advancements in different application fields ranging from precision surgery (*4*), advanced prosthetics (*5*), assistive devices (*6*), and fully implantable robots restoring physiological processes (*7*). Implantable robots should endow awareness of the body environment and action capabilities to favor proper integration with the human body and regulate biological and metabolic processes, in a closed-loop fashion as natural organs do (*8*). These implanted devices operate well beyond simple electric or mechanical stimulators. Despite being in its infancy, research on implantable robots has reported interesting results in the past years by offering new solutions for restoring lost organ functions or physiological processes, such as blood pumping (*9*), micturition (*10*), hormone delivery (*11*), and tissue regeneration (*12*).

Implantable robots can be of particular interest to address unmet clinical challenges. As an example, intraperitoneal insulin supply in people with type 1 diabetes (T1D) is of primary interest (*13*). The intraperitoneal route ensures a normal portosystemic insulin gradient, repositioning the liver as the physiologic initial target of insulin action and therefore limiting chronic peripheral hyperinsulinemia. At present, intraperitoneal delivery requires access devices (ports) connecting intraperitoneal catheters to external reservoirs or pumps (*14*, *15*). Complications such as obstruction of the catheter, infection, leakages, and pain are associated with intraperitoneal transcutaneous ports, thus causing delays in treatment, psychological burden, and high cost for the health care system (*16*). For all these reasons, despite advantageous metabolic effects, the intraperitoneal route has been little used for T1D treatment. An "all-on-board" fully implantable system for intraperitoneal delivery would avoid transcutaneous accesses and related complications. However, to enable this strategy, a means to refill the implanted reservoir upon shortage of drugs is mandatory. To this extent, the digestive system represents an interesting route for accessing internal organs or devices implanted in the abdominal cavity with minimal invasiveness. Smart ingestible capsules have been proposed in the state of the art as multifunctional systems for localized drug delivery (*17*, *18*). In this respect, they could also be exploited as drug carriers for refilling implanted reservoirs. Using the digestive system to access devices implanted in the abdominal cavity through smart drug-loaded ingestible capsules would allow noninvasive refilling of implanted devices and overcoming the complications associated with transcutaneous accesses.

Here, we describe PILLSID (PILl-refiLled implanted System for Intraperitoneal Delivery), a fully implantable device for intraperitoneal delivery. The device is grounded on a noninvasive refilling strategy based on ingestible magnetic pills carrying fresh drugs or hormones (e.g., insulin) to face the shortage of drugs due to prolonged use of the implanted system (*19*). Here, we report the prototyping and validation of PILLSID at the preclinical level. The efficiency of the proposed refilling strategy is demonstrated in vivo. When refilled with insulin, the microinfusion system was efficient and safe in regulating the blood glucose (BG) level in diabetic swine.

[1]BioRobotics Institute, Scuola Superiore Sant'Anna, Piazza Martiri della Libertà 33, 56127 Pisa, Italy. [2]Department of Excellence in Robotics & AI, Scuola Superiore Sant'Anna, Piazza Martiri della Libertà 33, 56127 Pisa, Italy. [3]Department of Mechanical and Automation Engineering, Chinese University of Hong Kong, Shatin NT, Hong Kong SAR. [4]Division of General and Transplant Surgery, Azienda Ospedaliera Universitaria Pisana, University of Pisa, Via Paradisa 2, 56124 Pisa, Italy. [5]Department of Clinical and Experimental Medicine, Section of Metabolic Diseases and Diabetes, University of Pisa, Via Savi 10, 56126 Pisa, Italy. [6]Emergency Surgery Unit, Azienda Ospedaliero Universitaria Pisana Cisanello Hospital, Via Piero Trivella, 56124 Pisa, Italy. [7]Dubai Future Labs, Dubai, United Arab Emirates. [8]Beijing Advanced Innovation Center for Intelligent Robots and Systems, Beijing Institute of Technology, Beijing, China. [9]Department of Mechanical Engineering, Tianjin University, Tianjin, China.
*Corresponding author. Email: arianna.menciassi@santannapisa.it
†These authors contributed equally to this work.

RESULTS

PILLSID is devised to be implanted in an extraperitoneal pouch fashioned between the costal margin and the iliac crest and delivers the target drug/hormone through an intraperitoneal catheter. The implantable system is surgically interfaced with the first jejunal loop in the left quadrant of the abdomen, immediately after the ligament of Treitz. The refilling procedure starts with drug-loaded capsule ingestion: The pill is passively transported along the gastrointestinal system by peristalsis until reaching the implant, where it is magnetically docked (Fig. 1A). After capsule docking, a small needle is ejected from the device, enabling the transfer of the hormone from the capsule to the implanted reservoir (Fig. 1B). Last, the pill is undocked and naturally excreted after running through the small intestine and the colon rectum.

Once refilled with drugs/hormones, the device acts as a programmable microinfusion system for precise intraperitoneal delivery. To guarantee safe and long-term operation, the system includes a telemetry system (Bluetooth communication protocol) allowing input/output exchange with a human-machine interface handled by the patient/clinician and a wirelessly rechargeable power source (i.e., a battery) (Fig. 1C).

PILLSID includes several operating blocks (Fig. 2) enabling the implementation of the described operative sequence. The docking mechanism represents a key component of PILLSID, because it allows the capture of the drug-loaded capsule transiting through the small bowel. This mechanism must guarantee efficient and stable capsule docking and should be robust to perturbations produced by intestine peristalsis and capsule punching. It should also be highly miniaturized to comply with implantability constraints as well as enable facile transition between the docked and released states. Inspired by industrial clamping systems (*20*) and pipe-inspecting robots (*21*), we designed a magnetic switchable device (MSD) working as a docking mechanism (*11*, *19*) for capturing magnetic capsules. By a 90° rotation of a permanent magnet within a stator made from ferromagnetic and diamagnetic materials, magnetic field streamlines can be redistributed to either activate or deactivate the attraction force over the docking surface. This kind of mechanism allows for a high force-to-volume ratio, low power consumption, and no need for perfect geometrical matching between the capsule and the docking surface, which are favorable for in vivo blind capsule capture.

Simulations predicted that a disc-shaped magnet (diameter 11 mm, thickness 5.5 mm, NdFeB, grade N52, diametrically magnetized) included in a custom nickel-iron–brass circuit (fig. S1) generates sufficient force to stably capture a 12-mm-diameter, 28-mm-long magnetic capsule (fig. S2) when parietal peritoneum and intestine tissue lie in between. This force drops down to almost zero when switching from the "ON" to the "OFF" state, thus guaranteeing capsule release (Fig. 3A).

Bench tests confirmed the simulated docking force values when interposing either a 1.3-mm silicone layer or ex vivo intestine tissue (about 1 mm thick) between the implantable device and the capsule (n = 5 per each experimental condition; Fig. 3B). A 23.4-mNm torque is needed to produce the 90° rotation of the magnet within the circuit, which is compatible with the output of a commercial dc micromotor (Faulhaber, 1512U003SR324:1 IE2-8, Germany) provided with a suitable reduction ratio (648:1). The docking force produced is almost 10-fold the capsule weight (along the z axis), about five times the capsule punching force (n = 5 per each experimental condition; along the x axis, Fig. 3, B and C), and substantially larger (seven times) than the average radial peristalsis force (*22*).

To advance from an intraluminal docking system to a fully implantable device appointed for intraperitoneal controlled delivery, several modules should be combined. In particular, the implementation

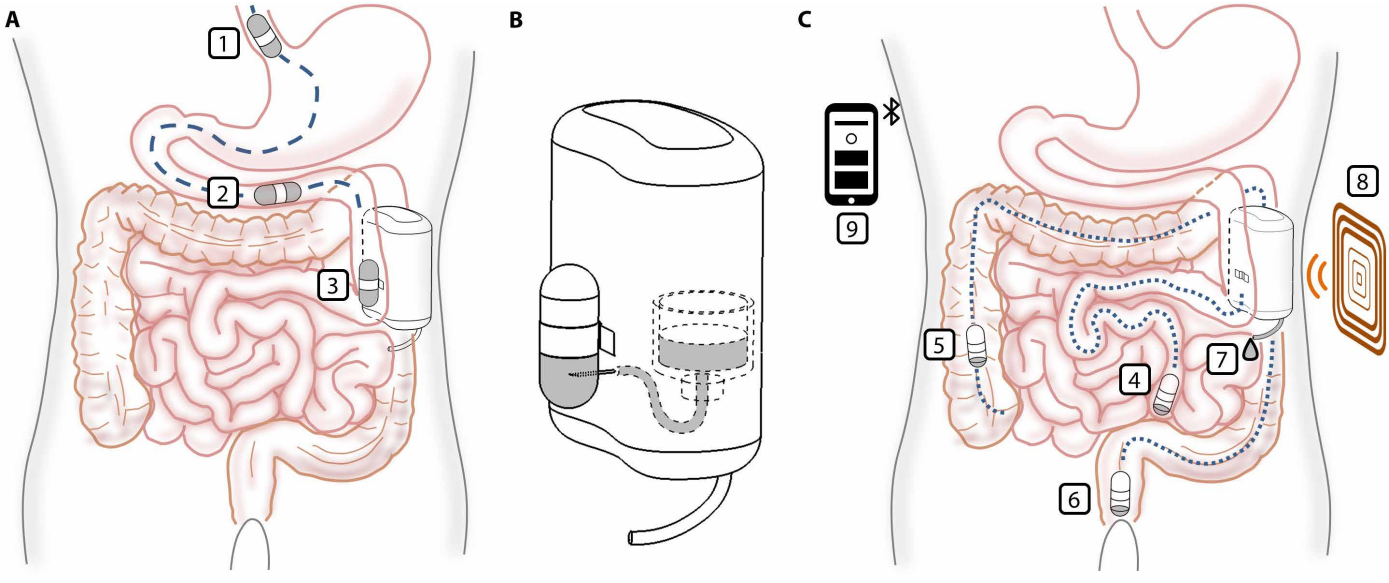

Fig. 1. PILLSID operation sequence overview. (**A**) The drug-loaded capsule is ingested by the patient (1) and passively advanced along the digestive system (2). When the capsule reaches the loop interfaced with the extraperitoneal pouch containing the device, it is magnetically docked (3). (**B**) The capsule is then punched by the retractable needle, and the drug contained in the pill is transferred to the reservoir of the implanted device. (**C**) The docking can then be deactivated to enable the capsule to be passed naturally through excretion (4 to 6). Once refilled, the implanted device acts as a microinfusion pump for intraperitoneal drug release (7). Wireless battery recharging (8) and Bluetooth-based communication with the implant (9) enable extended lifetime, safe device programming, and feedback exchange.

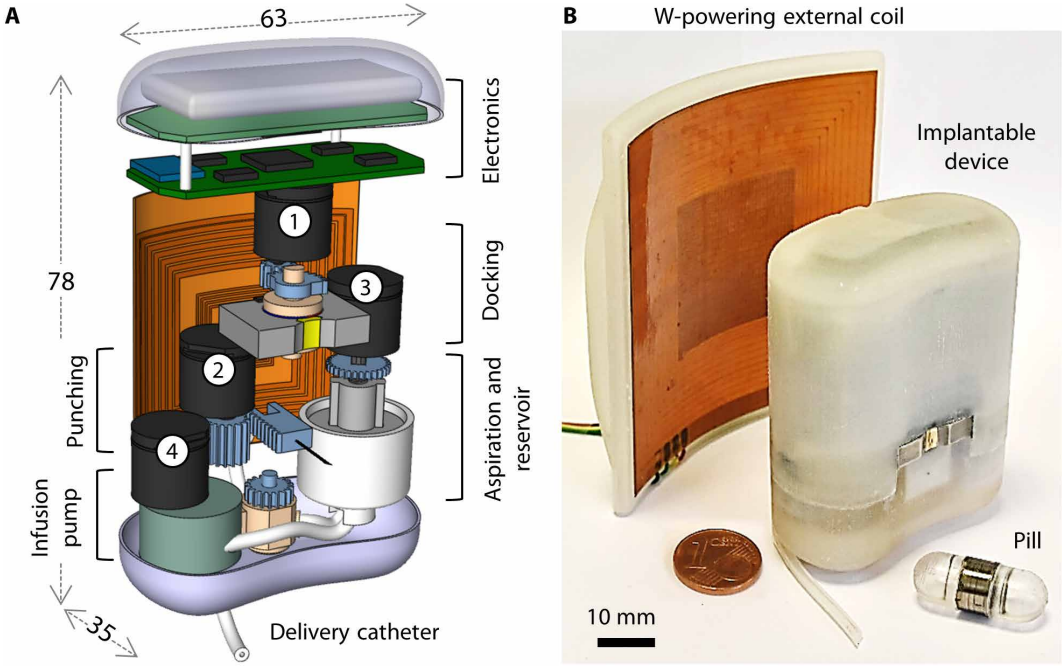

Fig. 2. PILLSID system schematic depiction and prototype. (**A**) The device includes four actuators (1, docking; 2, needle ejection; 3, variable volume reservoir; 4, infusion pump) and several operating blocks. Device measures are reported in millimeters. (**B**) The complete prototype includes the charging coil (W-powering external coil) and the pill, in addition to the implanted device. The implantable device has overall dimensions of 78 mm by 63 mm by 35 mm.

of the sequence depicted in Fig. 1 requires (i) a capsule punching/fluid aspiration module, (ii) a precise drug infusion system, (iii) a variable volume reservoir, and (iv) powering and control electronics for device management and interface with the user.

We used a 25-gauge needle mounted on a rack-pinion mechanism to enable needle linear ejection and capsule punching (fig. S3A). Needle and docking circuit relative positions were set to guarantee capsule punching irrespective of the exact capsule position (fig. S3B). The needle is connected to the reservoir through a medical-grade silicone tube. The reservoir is a variable volume Nylon system (*23*) provided with a linearly actuated plunger (fig. S4A). This structure has a double function: It creates a negative pressure favoring fluid drawing from the capsule, and it enables reservoir volume adjustment according to its drug content, thus minimizing air bubble formation. When targeting insulin delivery, it is particularly important to avoid drug interface with air to keep hormone stability and prevent aggregation. We experimentally observed that fluid aspiration from the pill occurs with a rate of 20 μl/s and that the reservoir refilling efficiency can vary in the range from 80 to 90% of the capsule content (corresponding to 1.24 to 1.39 ml transferred to the reservoir), when changing the device inclination with respect to gravity (n = 5 in each experimental condition). Refilling efficiency was validated also in vivo on a pig model (n = 3) and proved that 86.00 ± 6.56% of the capsule content (i.e., 1.33 ± 0.10 ml) transferred to the implanted reservoir (Fig. 3D). By design, the reservoir has separated inlet and outlet connected to the needle and to the microinfusion unit, respectively. This two-sided connection is regulated by a fluidic switch preventing undesired drug leakages from the needle (fig. S3C). The switch is coupled to the needle actuator: The aspiration line is open when the needle is ejected and closed when the needle is retracted, and no aspiration occurs. The microinfusion block relies on a six–rotating roller peristaltic pump operating in intermittent mode (fig. S4B). This pumping technology offers high resolution (i.e., the dose volume depends on the volume enclosed within the tube between two consecutive rollers), no contact between the mechanical components and the sterile fluid, and intrinsic behavior as a valve, preventing backflow and unintended leakages. The pump is designed to target a few microliter resolution to guarantee compatibility with highly concentrated formulations that would enable less frequent reservoir refilling procedures. Experimental validation proved a 3.18 ± 0.30–μl resolution irrespective of the time delay between consecutive ejections over repeated complete emptying cycles (n = 10 per each experimental condition; Fig. 3E). PILLSID is also provided with a wireless power transfer (WPT) strategy for leadless battery recharging. The WPT relies on electromagnetic coupling and consists of four coils printed on double-sided Kapton foils and operating in the 13.56-MHz medical band. The driver and transmitting coils represent the external unit worn by the participant and connected to a powering source, whereas the receiving and load coils are included in the implantable device and connected to the embedded battery through an integrated electronic circuit (fig. S5). In vitro characterization allowed verifying that when external and internal coils are perfectly coaxial and separated by 20 mm, the WPT efficiency can reach 53%. WPT efficiency varied with distance, curvature of the coils, and operating environment (Fig. 3F). WPT efficiency was demonstrated to be 44 ± 7% during in vivo validation in the curved configuration, which is optimal to guarantee good shape matching with the abdomen. This would guarantee a complete battery recharging in 4.5 hours with a standard 450-mAh lithium ion battery (table S1).

PILLSID mock-ups featuring three different shapes and three different volumes (Fig. 3G and fig. S6) were implanted in a human cadaver (male cadaver, n = 1). The test identified a kidney-shaped section (Fig. 3G, ii) with a 65-mm radius of curvature as the optimal geometry enabling safe interface with the intestine loop and optimal matching with the abdominal wall. We evaluated that the device volume should not exceed 150 to 160 mm^3 to allow implantation in an extraperitoneal pouch while limiting at the same time the dissected area, extraperitoneal bleeding, contact with the costal margin, and unaesthetic mass-forming effects. The specifications derived from the cadaver test enabled us to steer system optimization before in vivo testing. In addition, the cadaver test allowed to define the

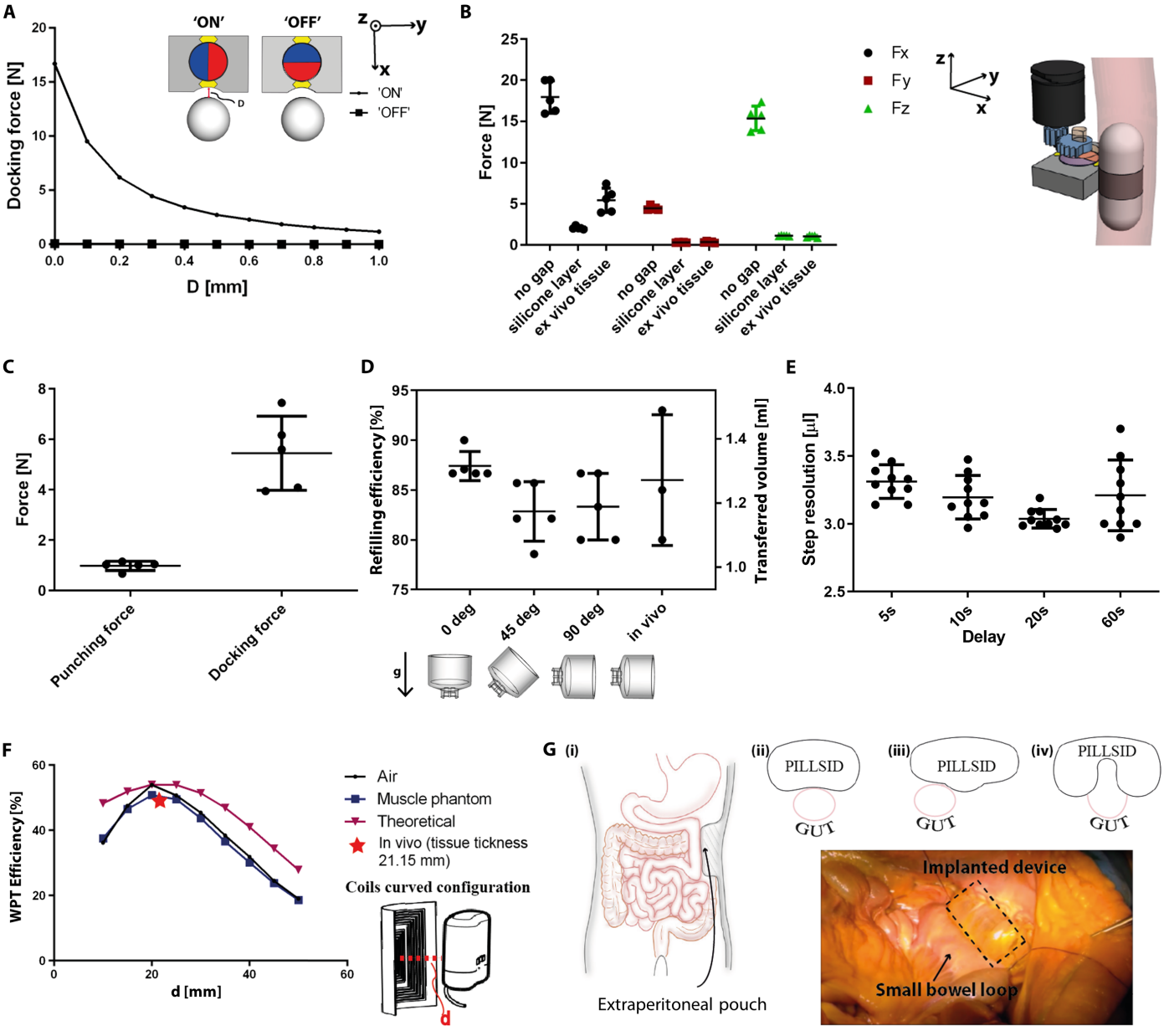

Fig. 3. Key performance of PILLSID blocks. (**A**) Simulated docking force in the ON and OFF configurations. (**B**) Experimental magnetic docking force along the three main axes when varying the medium interposed between the MSD and the capsule. (**C**) Comparison between the docking and punching forces under ex vivo conditions. (**D**) Refilling efficiency in vitro and in vivo for different reservoir orientations. (**E**) Pump resolution when varying delays among consecutive ejections. (**F**) WPT efficiency in vitro across different media and in vivo. Depiction of the device and external coil relative positioning. (**G**) Definition of the implant procedure and device shape and size through cadaver laboratory testing. In (B) to (E), the points represent the experimental values, and the bars represent the mean and the SD of $N = 3$ to 10 measurements in the same set.

surgical procedure required for extraperitoneal pouch creation, device implantation, intestine loop displacement, and interface with the docking system.

We tested PILLSID on diabetic pigs ($n = 3$) by using short-acting human insulin as a drug model. Differently from the cadaver test, the device was implanted in the right quadrant to guarantee better iliac loop displacement based on the anatomical differences between the two experimental models (figs. S7 and S8). Transit tests revealed that our capsule takes about 4 days in the animal model to naturally reach the device implant area if moved by peristalsis only. A subcutaneous commercial glucose sensor combined with a near-field communication (NFC)–Bluetooth transducer was implanted at the neck level for continuous BG monitoring (Fig. 4A). Upon implantation, the entire PILLSID operation sequence reported in Fig. 1 was successfully validated. Fluoroscopic monitoring allowed us to verify successful capsule approaching, docking, and punching and to prove capsule-docking stability during the punching phase (Fig. 4B). Successful docking was also verified through an on-board

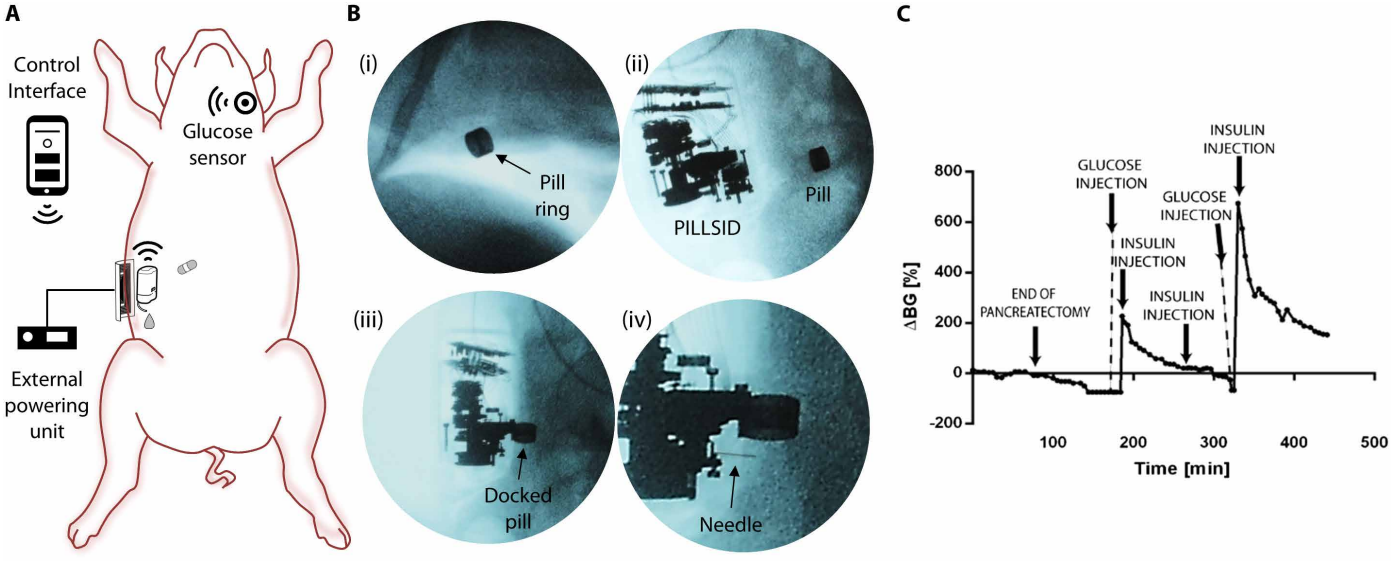

Fig. 4. PILLSID in vivo testing. (**A**) Experiment setup overview. (**B**) Fluoroscopic monitoring of the implanted reservoir refilling procedure: (i) The capsule is in the stomach and progressively advances to reach the small bowel (ii). The capsule approaches the device; it is stably docked (iii) and punched (iv). (**C**) PILLSID in vivo testing in diabetic swine. The device successfully released intraperitoneal controlled doses of insulin, enabling BG level regulation. The reported plot refers to one of the three pigs and aims at showing BG level trend upon PILLSID operation.

magnetic field sensor placed on the MSD circuit (fig. S9). The sensor detects the magnetic field variations induced by streamline redistribution upon switching between ON and OFF configurations and upon capsule docking. Type 3C diabetes mellitus was induced in the pigs through total pancreatectomy. We demonstrated that the implantable device could control the insulin release intraperitoneally, thus enabling BG level regulation and normoglycemia recovery (Fig. 4C). We also verified that upon intravenous glucose injection as in standard tolerance tests, the microinfusion pump decreases the BG level at a repeatable rate ($\frac{\Delta BG}{IU * min} = 0.10 \pm 0.03$ mg dl^{-1} IU^{-1} min^{-1}).

DISCUSSION

The results reported here demonstrate that a fully implantable robotic device provided with a reservoir can be noninvasively refilled through magnetic pills carrying insulin. Once refilled, the device proved efficient in regulating the BG level in a diabetic swine by intraperitoneal insulin infusion. Wireless data transfer to a human-machine interface and wireless battery recharging were successfully demonstrated, enabling device handling, commands/feedbacks exchange, and prolonged powering. PILLSID represents a step forward in the fields of both implantable medical devices and intraperitoneal delivery. Few implantable insulin pumps for intraperitoneal delivery have reached the clinical trial stage and have been launched on the market so far. However, these pumps are currently little used in clinical practice due to catheter failure, short battery lifetime, and need to perform reservoir refilling in hospital settings by a trained nurse (*24*). The device proposed here presents weight (165 g) and dimensions (78 mm by 63 mm by 35 mm) comparable with those of the aforementioned pumps and other implantable medical devices, but it solves some critical issues like those related to reservoir refilling and powering.

If provided with a proper adaptive control algorithm (*25*) and combined with a glucose sensor, PILLSID could also be eligible as the first fully implantable artificial pancreas system. Given the volume of the capsule, the person with diabetes will be requested to ingest an insulin capsule every 4, 9, or 21 days depending on the selected insulin concentration (U100, U200, or U500, respectively). This would represent an advancement with respect to traditional insulin therapy (which implies multiple injections and blood stick every day) or wearable insulin pumps requiring continuous supervision.

Although type 2 diabetes could be a potential target for a system like the one presented here, the insulin deficiency characterizing T1D makes this form of diabetes the natural condition to be tackled, particularly in light of a closed-loop system. A relatively small percentage of patients affected by type 2 diabetes and with intensive insulin therapy needs may also benefit from this device. However, given the need for surgery to implement the proposed therapeutic strategy, the typical age of patients with type 2 diabetes, and their less demanding exogenous insulin need, the main clinical target remains T1D. Intraperitoneal delivery through an implantable system might also stand as particularly advantageous in the acute pharmacological treatment of metastatic tumors in the peritoneal cavity (e.g., ovarian, pancreatic, gastric, and colorectal cancers) (*26*). Ideally, PILLSID could allow a long-term release of intraperitoneal chemotherapy simulating the classical intravenous infusion protocol but with the advantages of the intraperitoneal diffusion. This would enable overcoming the side effects of the one-shot approach, programming the release kinetics, and allowing a notable reduction in doses, thus in potential side effects (*27*, *28*).

Given the complexity of the system, several additional steps are required to let the system reach clinical practice. As for every medical device, once the feasibility and efficacy of the approach are demonstrated, as reported here, a detailed risk analysis should be performed to assess the robustness and reliability of the system toward a more extensive validation. Risks related to unsuccessful punching or docking, as well as catheter obstruction, should be taken into account in the future while optimizing the PILLSID design.

To mitigate some of these risks, the device might be provided with additional sensors and on-board intelligence to detect failure events. This could entail the use of flow sensors for pump and reservoir monitoring, current reading circuits for punching verification, dedicated sensors to track capsule approaching, etc. Additional efforts should also be made to render the system more robust (e.g., in terms of docking stability) and safer, in terms of interaction with the host. This effort would imply minimizing localized stress due to repeated punching and minimizing adverse immune reaction by a more careful materials selection.

Last but not least, given the site of implantation and the current features of the device (size, powering technology, docking force, etc.), interparticipant differences still represent a decisive variable for PILLSID operation and suitability. For example, the device might not be suitable for children/adolescents because of its size and might perform differently in terms of powering performances based on patient build. Although there remain outstanding challenges, the results reported here lay the foundations for the generation of fully autonomous, refillable, and implantable devices for chronic and life-threatening pathology treatment.

MATERIALS AND METHODS

Docking circuit

A single-magnet MSD circuit was designed on the basis of previous results reported by the authors (*11*), and finite element method (FEM)–based simulations were carried out in Comsol Multiphysics environment (ac/dc module and static magnetic field conditions). The aims were maximizing the attraction force exerted on the ingestible pill and guaranteeing fast and efficient transition between OFF and ON configurations. An N52 diametrically magnetized disc-shaped permanent magnet (11 mm diameter, 5.5 mm thick; Alga Magneti, Italy) acts as a rotor, whereas two ferromagnetic u-shaped parts soldered together with brass constitute the circuit stator. A 100-μm air gap separates the rotor and the stator to favor reciprocal rotation. A commercial iron-nickel alloy (Ed Fagan, Efy Alloy 50) proved optimal for fabricating the stator components and the pill magnetic ring via computer numerical control machining center for microfabrication (Kern HSPC) and a wire electric discharge machine (SODIC AP200L). The overall MSD system is 23.5 mm by 16.5 mm by 5.5 mm, thus guaranteeing optimal integration within the overall device. When the MSD is ON, the streamlines cross the device circuit surface, thus generating an attraction force on the ferromagnetic ring surrounding the pill (fig. S1). In this configuration, the pill docking force is theoretically suitable to guarantee stable docking against physiological disturbances. In the OFF configuration, streamlines go directly through the two u-shaped stator parts without crossing the active surface, thus without attracting the ferromagnetic ring but instead releasing it.

The magnet is connected on opposite sides with two shafts blocked by ball bearings for stable assembly, rotation, and perfect coaxiality between the stator and the rotor. The top shaft is also connected to a spur gear (provided with teeth only over a 90° section to save space) featured by a 2:1 reduction ratio to produce magnet rotation by a dc micromotor (Faulhaber 1512U003SR324:1 IE2-8, motor 1; Fig. 2).

A magnetic field (Hall effect) sensor is mounted on the ferromagnetic circuit to sense local variations of magnetic field associated with the capsule docking event. FEM simulations were carried out to derive a map of the magnetic field normal component variation over the stator surface, upon transition between the two capsule configurations (docked and undocked). Simulations allowed us to identify the regions of maximum variations (up to 100 mT) for optimal sensor positioning (fig. S9). A compact analog Hall sensor (Sonnecy, CYSJ902, Germany) was selected because of its wide operating range (0 to 2 T) and good sensitivity (0.5 mV/mT with a 3.3-V power supply), which is able to produce a 50-mV step signal upon docking event when the sensor is placed in a maximum field variation node. This signal can be detected by a threshold recognition routine implemented in the microcontroller and can be interpreted as a successful docking flag for controlling the aspiration unit timing (see the Supplementary Materials for validation procedure).

Punching and aspiration

The aspiration block includes the linear punching system, a fluidic switch, and a variable volume reservoir. A dc Faulhaber rotary motor (1512U003SR324:1 IE2-8, motor 2; Fig. 2) connected to a rack-pinion mechanism was used for the linear actuation of the needle (fig. S3A). The rack-pinion mechanism includes a toothed pinion (n = 18, module 0.5) connected to a rack of the same module to allow the transmission of motion from the motor to the needle.

Selecting the right needle size was essential to guarantee acceptable drug/hormone flow, complete retraction of the needle inside the device, and correct punching of the capsule while minimizing the lesion produced on tissue by punching. A 25-gauge needle was selected, guaranteeing short aspiration time (about 3 min).

A medical-grade silicone tube (inner diameter, 1 mm; PR410/40, Primasil Ltd., Herefordshire, UK) connects the needle to the reservoir by passing through the rack and through the custom fluidic switch. The switch prevents undesired leakages and backflow: It is kept open during the aspiration phase and closed for the rest of the time, thus avoiding undesired drug leakage from the needle. The switch is mechanically coupled with the needle: A shaft is connected to the punching pinion through a spur gear pair (18 teeth, module 0.5), thus compressing the aspiration line tube when the needle is in the retracted configuration (thus when no aspiration occurs) (fig. S3C).

The aspiration block also includes the variable volume reservoir. Reservoir volume varies with insulin content to avoid the drug contacting air, thus favoring its stability. To enable internal volume variations, the reservoir is designed as a syringe featured by a linearly actuated plunger. This structure also enables to create a negative pressure in the reservoir upon plunger pullout so as to facilitate fluid aspiration from the needle. A cylindrical reservoir featured by a conical-shaped terminal part was fabricated from Nylon 6 to not hamper insulin stability (*23*). The reservoir (fig. S4A) has a volume of 2.5 ml and includes two openings in the terminal part to guarantee connection to the needle and to the pump. The plunger includes a Fluorosilicone O-ring (Apple Rubber, New York, USA) for better sealing and is actuated by a dc Faulhaber motor (the same used for the other actuation mechanisms, motor 3 in Fig. 2) and a metallic spur gear pair (1:2.5 reduction ratio to maximize its force). The gear is attached to a threaded shaft (stainless steel, M4) and to a ball bearing on top. The plunger is centrally threaded (M4) to move inside the reservoir through a screw mechanism. By providing a sliding channel on the external fixture, the rotary motion of the motor is converted to a bidirectional translational movement on the plunger (fig. S4A). The plunger is three-dimensionally (3D) printed in stainless steel (DMLS/SLM by ZARE srl, Italy), whereas the

remaining components were 3D printed in VisiJet M3 crystal (ProJet MJP3600, 3D Systems, USA) (see the Supplementary Materials for validation procedure).

Pump unit

A rotary peristaltic pump operating in intermittent mode was designed and developed to achieve a few microliter resolution while avoiding direct contact between the pumped fluid and microinfusion system mechanical components, thus preventing contamination. By design, the dose of fluid interposed between consecutive rollers advances upon rotation. The rollers normally compress the tube, thus preventing backflow and undesired leakages. The dose, thus the pump resolution, is determined by the number of rollers and by the tube size. By design, a single dose ejection is produced by a rotation equal to $2\pi/n$, where n is the number of rollers. On the basis of preliminary pump designs developed by the authors (*29*), an infusion system with six rotating rollers was developed. The rollers were designed with gears (10 teeth, module 0.4; fig. S4B) on the bottom side to be engaged by a pinion gear (12 teeth, module 0.4). All rollers are caged together by the rotor to allow their engaging with the pinion and their rotation with the same speed by exploiting the torque produced by a dc micromotor (Faulhaber 1512U003SR324:1 IE2-8, motor 4; Fig. 2). The designed pump includes six rollers for an overall 20-cm^3 volume and theoretically enables the delivery of 3-μl doses. In the proposed pump, the tube is the only component entering in contact with the fluid and should be made of a material that is chemically compatible with the drug of interest and biocompatible because it enters in touch with the peritoneum. Furthermore, it should feature specific mechanical properties combining at the same time high flexibility and high resistance to cyclical mechanical stresses, thus keeping the circular cross section stable upon repeated pump cycles. This led us to choose a medical-grade silicone tube (PR 410/40, Primasil Ltd., Herefordshire, UK) (see the Supplementary Materials for validation procedure).

Pill

The drug-loaded capsule should comply with a set of specifications aimed at guaranteeing painless and safe capsule ingestion, resistance to the acidic gastrointestinal environment, suitable magnetic properties to enable stable docking, and favorable mechanical properties to allow easy punching. Capsule dimensions were defined (diameter, 12 mm; length, 28 mm) in agreement with those of commercial systems for painless colonoscopy (*30*), considered as the largest pills to be easily and safely swallowed by a human participant. By design, the capsule consists of three parts: two identical polymeric caps held together by a ferromagnetic ring intended for docking. Polydimethylsiloxane (PDMS; Sylgard 184) was selected as the polymeric matrix in light of its easy fabrication through molding, mechanical properties tunability, and resistance to acidic environments. Dedicated molds were designed and fabricated by Teflon, thus obtaining 1-mm-thick capsule walls while using PDMS 10:1 monomer:curing agent ratio (fig. S2B). The three capsule components were glued together by exploiting the internal ferromagnetic ring surface and filled with the target drug upon assembly by means of a 31-gauge needle syringe. The capsule load capacity is 1.55 ml.

Wireless power transfer

The WPT system stands on magnetic coupling between two coils, one acting as a transmitter and the other as a receiver. The received current is modulated to charge a battery or directly operating electronic components. Printed spiral coils allow enhanced mutual inductance and higher reactive impedance (Q factor) with respect to wire-wound coils, thus leading to a more efficient inductive power transmission (*31*). Recently, four-coil systems (two coils in the transmitting unit and two coils in the receiving one) have been proposed (*32*) to achieve better power transfer efficiency (PTE) especially for relatively high distances among the coils. In this configuration (that was selected in the PILLSID wireless powering system), all the coils are tuned at the same resonance frequency by dimensioning the capacitors placed in series with the coils. The resonance frequency is typically chosen on the basis of the desired working distance and on the working environment. In the specific case of in-body applications, international standards and safety indications for absorbed radiation dose should be taken into account when selecting the magnetic field intensity and the operating resonant frequency (*33*).

An iterative design process has been followed toward PTE optimization. The iterative design process was carried out by taking into account the dimensional constraints imposed by the device [e.g., outer diameter (D_o)] and the fabrication technology constraints [e.g., minimum conductor width (w) and spacing (s)] (*34*). At each step, w and the number of turns (n) are fixed, whereas the coupling and Q factor (*31*) are calculated in MATLAB software to analyze how efficiency varies with distance between coils. The optimization process continues by calculating inductance (L), parasitic resistor and capacitance at the resonant frequency (13.56 MHz) reaching optimal width, n-turns, thickness (t), and internal diameter (D_i) of each of the four coils. The optimization process led to the definition of the coil specification (table S2).

Coils are made of double-sided flexible Kapton printed circuit boards (fig. S5). The external coil (Tx), consisting of driver plus primary coil, is connected to the ac signal generator and power amplifier outside the body. The internal coil (Rx), consisting of secondary plus load coil, has been sized to link with the generated external field and to transfer the received power to the load (i.e., battery plus dedicated circuitry) (see the Supplementary Materials for validation procedure).

Control electronics

Control electronics was organized into two stacked boards, dedicated to sensors/actuators control (Micro board) and to power management (Powering board), respectively (fig. S5B), to comply with space constraints. The Micro board hosts the central microcontroller and additional crystals, capacitors, and resistors for optimal sensors and actuators operation. It also encloses motor drivers, power switches, and the Bluetooth module to guarantee data exchange with the human-machine interface. The Powering board hosts a charging module, a charge detector, and a voltage converter. These two boards are connected by six lines of voltage-data communication and stacked through dedicated spacers. The electronic boards are kept on the top of the dc motors to favor easier electrical connections.

To guarantee position control of the four dc motors included in the device, each motor is connected to a driver, a power switch, and the microcontroller. The driver chips (DRV8833, Texas Instruments, USA) are provided with power switches (TPS22860, Texas Instruments, USA) to ensure correct powering of the motors, to enable/disable the power supply line of the encoders, and to reduce power consumption. The optical encoders integrated into the selected dc micromotors are connected to microcontroller timer/counters to

monitor motor operation. An automatic voltage regulator (AVR) microcontroller ATMega324PB (Microchip, USA) was selected for this purpose in light of the suitable number of timer/counters. The microcontroller also communicates with an external user interface (i.e., a tablet) to receive commands and to send status information of PILLSID units (such as reservoir level, infusion history, and battery percentage) via a Low Energy Bluetooth module (BLE 652, Laird, USA). The microcontroller also collects the data of the Hall sensor by analog-to-digital converter (ADC) pins and transfers the measured values to the user's tablet via Bluetooth. It can keep timing between successive infusions to inject insulin by a recommended routine in the loop. All necessary status variables are saved in the microcontroller electrically erasable programmable read-only memory (EEPROM) to prevent data loss due to unexpected accidental reset events.

Dedicated electronics was used also for power management and for recharging the implanted battery by modulation of the power transmitted by the Tx coils to the Rx ones. A wireless charging module (LTC4120, Linear Technology) and specific electronic circuitry are used to rectify and modulate the ac current signal in the control board. A gauss gauge (LTC2942, Linear Technology) allows monitoring of the battery charge level and information transmission to the microcontroller. Moreover, a dc-dc buck-boost converter enables modulating and adapting the battery voltage to that required by the microcontroller and dc motors.

Cadaver procedure

The abdomen was opened through a midline incision. The ideal intestinal loop was selected in the left quadrant of the abdomen, after the ligament of Treitz, where the first jejunal loop can be approximated to the abdominal wall with a shorter path. The pouch should be fashioned in between the costal margin and the iliac crest where the abdominal wall is rather elastic. To avoid the device pressing on a rigid plane and a mass-forming effect on the abdominal wall, device size should be within a specific limit.

The pouch was created by blunt dissection, and the device was introduced in it. The delivery catheter was moved intraperitoneally through a small hole in the pouch. The extraperitoneal pouch was then closed with a reabsorbable running suture. We tested on the cadaver three different device volumes and three different geometries (fig. S6) to identify the most suitable one to avoid mass-forming effects in the abdomen while guaranteeing proper pouch creation and suture. The jejunal loop was fixed to the extraperitoneal pouch at the level of the device concavity with two sutures running in parallel.

In vivo testing

All animal experiments were approved by the Italian Ministry of Health (protocol no. 65E5B.33). Swine (*Sus scrofa domesticus*, $n = 3$, males, weight of about 30 kg, no specific inclusion criteria were adopted) was selected as the animal model because of the anatomical similarities of the gastrointestinal system with humans and comparable glucose-insulin metabolism. Swine were fasted 24 hours before starting the test. A single experimental group was considered to reduce the number of animals used. Baselines were evaluated before starting the surgical procedure and before activating the device to obtain reference values.

Fashioning of the extraperitoneal pouch

On the basis of the anatomical differences among humans and swine, we opted for positioning the device on the right flank. By following the concept learned on the human cadaver, the extraperitoneal pouch was created by blunt dissection (fig. S7A), and the peritoneum was kept completely intact.

The pouch should not be excessively wide but should perfectly fit the device both to avoid possible migration during the first period after the implantation and to avoid additional sutures. A small incision was performed in the peritoneum to move the releasing catheter intraperitoneally (fig. S7B). The pouch was closed with a running suture of 2/0 polydioxanone (fig. S7C).

Intestinal loop fixation and refilling of the device

The intestinal loop was placed in position, at the level of the concave docking site of the device, through two 4/0 polydioxanone stay sutures. Differently from the cadaver, we opted for fixing the loop with two layers (anterior and posterior) of cyanoacrylate glue deposited on the antimesenteric face of the bowel (fig. S8). The connection created by cyanoacrylate could be more homogeneous and uniform compared with the running suture. The cyanoacrylate must not be placed at the level of needle ejection to avoid refilling procedure failure.

The intestinal loop was opened 20 cm before the docking site to allow insulin-filled (human regular insulin, U100) capsule insertion. The incision was closed with a running suture of 4/0 polydioxanone. Because of anesthesia, natural peristalsis results substantially slowed down, preventing capsule advancement. Neostigmine methylsulfate (0.5 mg/ml, 3 ml) was intravenously administered to improve the peristaltic wave and shorten the transit time while trying to reproduce natural peristalsis.

Insulin release

A total pancreatectomy was performed to rapidly induce diabetes mellitus. After total pancreatectomy, glycemia slowly fell down as a consequence of the swine fasting. The swine was intravenously administered with 20 ml of 50% dextrose solution (10 g) to speed up the rise of the glycemia. Fifteen minutes later, BG level was about 160 mg/dl, and 10 IU of insulin (corresponding to about 30 pump steps) was delivered intraperitoneally. To further test insulin release from the device, a second dextrose dose was administered to the pig (50 ml of 50% dextrose solution) to produce a rapid rise in BG level. BG rise was followed by a second insulin bolus (25 IU, 83 pump steps) delivered by the implanted PILLSID to restore normoglycemia.

The glycemia was monitored both through ear stick (performed every 10 min) and through a subcutaneous Abbott Freestyle Libre sensor. BG was represented and evaluated in terms of BG variation with respect to the basal level (Fig. 4C) and in terms of rate of BG variation per injected unit of insulin and per unit of time. The recorded data were postprocessed in MATLAB software.

SUPPLEMENTARY MATERIALS

robotics.sciencemag.org/cgi/content/full/6/57/eabh3328/DC1
Supplementary Text
Figs. S1 to S10
Tables S1 and S2
MDAR checklist

REFERENCES AND NOTES

1. G.-Z. Yang, R. Riener, P. Dario, To integrate and to empower: Robots for rehabilitation and assistance. *Sci. Robot.* **2**, eaan5593 (2017).
2. G.-Z. Yang, J. Cambias, K. Cleary, E. Daimler, J. Drake, P. E. Dupont, N. Hata, P. Kazanzides, S. Martel, R. V. Patel, V. J. Santos, R. H. Taylor, Medical robotics—Regulatory, ethical, and legal considerations for increasing levels of autonomy. *Sci. Robot.* **2**, eaam8638 (2017).

3. A. Gao, R. R. Murphy, W. Chen, G. Dagnino, P. Fischer, M. G. Gutierrez, D. Kundrat, B. J. Nelson, N. Shamsudhin, H. Su, J. Xia, A. Zemmar, D. Zhang, C. Wang, G.-Z. Yang, Progress in robotics for combating infectious diseases. *Sci. Robot.* **6**, eabf1462 (2021).
4. G. Fagogenis, M. Mencattelli, Z. Machaidze, B. Rosa, K. Price, F. Wu, V. Weixler, M. Saeed, J. E. Mayer, P. E. Dupont, Autonomous robotic intracardiac catheter navigation using haptic vision. *Sci. Robot.* **4**, eaaw1977 (2019).
5. E. D'Anna, G. Valle, A. Mazzoni, I. Strauss, F. Iberite, J. Patton, F. M. Petrini, S. Raspopovic, G. Granata, R. Di Iorio, M. Controzzi, C. Cipriani, T. Stieglitz, P. M. Rossini, S. Micera, A closed-loop hand prosthesis with simultaneous intraneural tactile and position feedback. *Sci. Robot.* **4**, eaau8892 (2019).
6. Y. Ding, M. Kim, S. Kuindersma, C. J. Walsh, Human-in-the-loop optimization of hip assistance with a soft exosuit during walking. *Sci. Robot.* **3**, eaar5438 (2018).
7. G.-Z. Yang, J. Bellingham, P. E. Dupont, P. Fischer, L. Floridi, R. Full, N. Jacobstein, V. Kumar, M. McNutt, R. Merrifield, B. J. Nelson, B. Scassellati, M. Taddeo, R. Taylor, M. Veloso, Z. L. Wang, R. Wood, The grand challenges of *Science Robotics*. *Sci. Robot.* **3**, eaar7650 (2018).
8. A. Menciassi, V. Iacovacci, Implantable biorobotic organs. *APL Bioeng.* **4**, 040402 (2020).
9. E. T. Roche, M. A. Horvath, I. Wamala, A. Alazmani, S.-E. Song, W. Whyte, Z. Machaidze, C. J. Payne, J. C. Weaver, G. Fishbein, J. Kuebler, N. V. Vasilyev, D. J. Mooney, F. A. Pigula, C. J. Walsh, Soft robotic sleeve supports heart function. *Sci. Transl. Med.* **9**, eaaf3925 (2017).
10. T. Mazzocchi, L. Ricotti, N. Pinzi, A. Menciassi, Magnetically controlled endourethral artificial urinary sphincter. *Ann. Biomed. Eng.* **45**, 1181–1193 (2017).
11. V. Iacovacci, L. Ricotti, P. Dario, A. Menciassi, Design and development of a mechatronic system for noninvasive refilling of implantable artificial pancreas. *IEEE/ASME Trans. Mechatron.* **20**, 1160–1169 (2015).
12. D. D. Damian, K. Price, S. Arabagi, I. Berra, Z. Machaidze, S. Manjila, S. Shimada, A. Fabozzo, G. Arnal, D. Van Story, J. D. Goldsmith, A. T. Agoston, C. Kim, R. W. Jennings, P. D. Ngo, M. Manfredi, P. E. Dupont, In vivo tissue regeneration with robotic implants. *Sci. Robot.* **3**, eaaq0018 (2018).
13. E. Renard, Insulin delivery route for the artificial pancreas: Subcutaneous, intraperitoneal, or intravenous? Pros and cons. *J. Diabetes Sci. Technol.* **2**, 735–738 (2008).
14. A. Liebl, R. Hoogma, E. Renard, P. H. L. M. Geelhoed-Duijvestijn, E. Klein, J. Diglas, L. Kessler, V. Melki, P. Diem, J.-M. Brun, P. Schaepelynck-Bélicar, T. Frei; European DiaPort Study Group, A reduction in severe hypoglycaemia in type 1 diabetes in a randomized crossover study of continuous intraperitoneal compared with subcutaneous insulin infusion. *Diabetes. Obes. Metab.* **11**, 1001–1008 (2009).
15. L. Bally, H. Thabit, R. Hovorka, Finding the right route for insulin delivery – an overview of implantable pump therapy. *Expert Opin. Drug Deliv.* **14**, 1103–1111 (2017).
16. C. W. Helm, Ports and complications for intraperitoneal chemotherapy delivery. *BJOG* **119**, 150–159 (2012).
17. A. C. Anselmo, Y. Gokarn, S. Mitragotri, Non-invasive delivery strategies for biologics. *Nat. Rev. Drug Discov.* **18**, 19–40 (2019).
18. A. Abramson, E. Caffarel-Salvador, M. Khang, D. Dellal, D. Silverstein, Y. Gao, M. R. Frederiksen, A. Vegge, F. Hubálek, J. J. Water, A. V. Friderichsen, J. Fels, R. K. Kirk, C. Cleveland, J. Collins, S. Tamang, A. Hayward, T. Landh, S. T. Buckley, N. Roxhed, U. Rahbek, R. Langer, G. Traverso, An ingestible self-orienting system for oral delivery of macromolecules. *Science* **363**, 611–615 (2019).
19. L. Ricotti, T. Assaf, C. Stefanini, A. Menciassi, System for controlled administration of a substance from a human body-implanted infusion device, U.S. Patent 9,415,163 (2016).
20. J. M. D. Coey, Industrial applications of permanent magnetism. *Phys. Scr.* **T66**, 60–69 (1996).
21. M. Tavakoli, J. Lourenço, C. Viegas, P. Neto, A. T. de Almeida, The hybrid OmniClimber robot: Wheel based climbing, arm based plane transition, and switchable magnet adhesion. *Mechatronics* **36**, 136–146 (2016).
22. S. P. Woods, T. G. Constandinou, Wireless capsule endoscope for targeted drug delivery: Mechanics and design considerations. *IEEE Trans. Biomed. Eng.* **60**, 945–953 (2013).
23. V. Iacovacci, I. Tamadon, M. Rocchi, P. Dario, A. Menciassi, Toward dosing precision and insulin stability in an artificial pancreas system. *J. Med. Device* **13**, 011008 (2019).
24. H. Hanaire-Broutin, C. Broussolle, N. Jeandidier, E. Renard, B. Guerci, M.-J. Haardt, V. Lassmann-Vague; EVADIAC study group, Feasibility of intraperitoneal insulin therapy with programmable implantable pumps in IDDM: A multicenter study. *Diabetes Care* **18**, 388–392 (1995).
25. P. S. Thomas, B. Castro da Silva, A. G. Barto, S. Giguere, Y. Brun, E. Brunskill, Preventing undesirable behavior of intelligent machines. *Science* **366**, 999–1004 (2019).
26. Z. Lu, J. Wang, M. G. Wientjes, J. L.-S. Au, Intraperitoneal therapy for peritoneal cancer. *Future Oncol.* **6**, 1625–1641 (2010).
27. D. K. Armstrong, B. Bundy, L. Wenzel, H. Q. Huang, R. Baergen, S. Lele, L. J. Copeland, J. L. Walker, R. A. Burger, Intraperitoneal cisplatin and paclitaxel in ovarian cancer. *N. Engl. J. Med.* **354**, 34–43 (2006).
28. K. M. Stampler, D. O. Holtz, C. J. Dunton, Reducing excessive toxicity in ovarian cancer treatment: A personalized approach. *Future Oncol.* **7**, 789–798 (2011).
29. I. Tamadon, V. Simoni, V. Iacovacci, F. Vistoli, L. Ricotti, A. Menciassi, Miniaturized peristaltic rotary pump for non-continuous drug dosing, in *41st Annual International Conference of the IEEE Engineering in Medicine and Biology Society (EMBC)* (IEEE, 2019), pp. 5522–5526.
30. G. Ciuti, K. Skonieczna-Żydecka, W. Marlicz, V. Iacovacci, H. Liu, D. Stoyanov, A. Arezzo, M. Chiurazzi, E. Toth, H. Thorlacius, P. Dario, A. Koulaouzidis, Frontiers of robotic colonoscopy: A comprehensive review of robotic colonoscopes and technologies. *J. Clin. Med.* **9**, 1648 (2020).
31. U.-M. Jow, M. Ghovanloo, Design and optimization of printed spiral coils for efficient transcutaneous inductive power transmission. *IEEE Trans. Biomed. Circuits Syst.* **1**, 193–202 (2007).
32. A. K. RamRakhyani, S. Mirabbasi, M. Chiao, Design and optimization of resonance-based efficient wireless power delivery systems for biomedical implants. *IEEE Trans. Biomed. Circuits Syst.* **5**, 48–63 (2011).
33. A. S. Y. Poon, S. O'Driscoll, T. H. Meng, Optimal frequency for wireless power transmission into dispersive tissue. *IEEE Trans. Antennas Propag.* **58**, 1739–1750 (2010).
34. M. Schormans, V. Valente, A. Demosthenous, Practical inductive link design for biomedical wireless power transfer: A tutorial. *IEEE Trans. Biomed. Circuits Syst.* **12**, 1112–1130 (2018).

Acknowledgments: We thank D. Terlizzi and S. Burchielli from Centro Biomedicina Sperimentale, Gabriele Monasterio Foundation (Pisa) for help with in vivo porcine work and N. Funaro, A. Melani, and R. Di Leonardo from Scuola Superiore Sant'Anna mechanical and electronic workshops for help in component manufacturing and assembly. **Funding:** This work has been supported by the ROBO-IMPLANT project, funded by the Tuscany Region (PAR FAS 2007–2013, Bando FAS Salute 2014, CUP J82F17000050005). This research was also supported by the Italian Ministry of Education, Universities, and Research, PRIN Project "Forget Diabetes: Adaptive Physiological Artificial Pancreas (FORGETDIAB)" Prot. 2015PJ28EP.
Author contributions: V.I., I.T., L.R., F.V., and A.M. conceptualized the system. V.I., I.T., S.P., V.S., and L.M. designed and developed the implantable system prototype. I.T., S.P., V.S., and L.M. performed in vitro experiments. E.F.K., L.C., M.C., and F.V. devised and performed the surgical procedure. M.A. and S.D.P. designed the diabetes treatment experiments. V.I., I.T., V.S., E.F.K., L.C., L.R., F.V., and A.M. performed in vivo experiments. V.I. wrote the paper with contributions from I.T. and E.F.K. All authors discussed results and commented on and revised the manuscript. **Competing interests:** P.D., L.R., and A.M. hold a patent on a system for controlled administration of a substance from a human body–implanted device. The other authors declare no competing interests. **Data and materials availability:** All data needed to evaluate the conclusions in the paper are present in the paper or the Supplementary Materials.

Submitted 2 March 2021
Accepted 28 July 2021
Published 18 August 2021
10.1126/scirobotics.abh3328

Citation: V. Iacovacci, I. Tamadon, E. F. Kauffmann, S. Pane, V. Simoni, L. Marziale, M. Aragona, L. Cobuccio, M. Chiarugi, P. Dario, S. Del Prato, L. Ricotti, F. Vistoli, A. Menciassi, A fully implantable device for intraperitoneal drug delivery refilled by ingestible capsules. *Sci. Robot.* **6**, eabh3328 (2021).

Science Robotics

A fully implantable device for intraperitoneal drug delivery refilled by ingestible capsules

Veronica Iacovacci, Izadyar Tamadon, Emanuele Federico Kauffmann, Stefano Pane, Virginia Simoni, Leonardo Marziale, Michele Aragona, Luigi Cobuccio, Massimo Chiarugi, Paolo Dario, Stefano Del Prato, Leonardo Ricotti, Fabio Vistoli, and Arianna Menciassi

Sci. Robot. **6** (57), eabh3328. DOI: 10.1126/scirobotics.abh3328

Science Robotics (ISSN 2470-9476) is published by the American Association for the Advancement of Science. 1200 New York Avenue NW, Washington, DC 20005. The title *Science Robotics* is a registered trademark of AAAS.